EASR

Engineering and Applied Science Research

https://www.tci-thaijo.org/index.php/easr/index

Published by the Faculty of Engineering, Khon Kaen University, Thailand

Water vapor barrier property of PLA nanocomposites using rice husk ash and layered double hydroxides as fillers

Chuenkhwan Tipachan[1)], Rakesh K. Gupta[2)] and Somjai Kajorncheappunngam*[1)]

[1)]Department of Chemical Engineering, Faculty of Engineering, Khon Kean University, Khon Kaen 40002, Thailand
[2)]Department of Chemical and Biomedical Engineering, West Virginia University, Morgantown, WV 26506, USA

Received 26 February 2019
Revised 31 May 2019
Accepted 18 June 2019

Abstract

Biodegradable polylactic acid (PLA) nanocomposite films with organically modified nanoclay (PKL_DS) and silica from rice husk ash (SiRHA) incorporation were prepared using a solvent casting method. The morphology and water vapor transmission rate behavior of these PLA based nanocomposite films with the addition of PKL_DS and SiRHA fillers was investigated at various loadings. The morphology of the nanocomposite was examined using X-ray diffraction (XRD), transmission electron microscopy (TEM) and scanning electron microscopy (SEM). It was confirmed that PLA molecular chains were intercalated into the interlayers of nanoclay (PKL_DS), which was well dispersed in the PLA matrix. TEM results showed SiRHA agglomerates and poor dispersion. The scanning electron microscopy (SEM) results showed good dispersion and good compatibility between nanoclay (PKL_DS) and the PLA matrix, while the SiRHA filler exhibited phase separation, silica agglomeration and some pore structures in the PLA matrix. The surface of the nanocomposite film with the incorporation of a SiRHA/PKL_DS combination exhibited a dense structure. A maximum reduction of 67% of water vapor transmission rate (WVTR) was obtained for nanocomposite films with co-addition of 10 wt% PKL_DS and 3 wt% SiRHA over that of PLA alone. It is concluded that the incorporation of a SiRHA/PKL_DS combination was very effective in improving the water vapor barrier property of a PLA based nanocomposite.

Keywords: Poly(lactic acid), Nanocomposite, LDH clay, Silica rice husk ash, Water vapor barrier

1. Introduction

For years, developments have been made to improve the properties and performance of plastic packaging. Plastic packaging that has been used to retard gas and water vapor permeation in particular has benefited from technological advancements. The result is that one can now have packaging, such as active packaging, which prevents contact with external vapor or moisture, extending the shelf life of food and preventing food waste. Packaging has also benefited from research on nanocomposite polymer materials. Some of these utilize inorganic compounds on a nanometer scale and have various chemical properties and morphological characteristics. When mixed with other polymers, they create plastics that prevent gas and/or water vapor permeation. For example, adding nanoclay layered double hydroxides (LDH) to poly(lactic acid) (PLA) to be used as a coating was found to form a PLA/nanoclay LDH composite with as much as a 35 % reduction in water vapor permeability [1]. Additionally, Shankar et al. [2] studied the effects of nano-particle size on the water vapor permeability through a PLA/zinc oxide nanocomposite film. It was reported that the water vapor permeability decreased by 30.5% when 0.5 wt% of zinc oxide was added. There are few studies focusing on the influence of silica from rice husk ash on the water vapor barrier properties of PLA-based composite films. Most of the PLA-based nanocomposite studies are related to PLA/layered nanoparticles. However, silica nanoparticles are of interest due to their natural abundance, low cost, high thermal resistance, surface functionality and suitability for various applications [3]. Among the investigations on the influence of silica nanoparticles on PLA properties is the work of Masnar and Coorey [4] who examined a PLA/silica from a rice husk ash/Sago pith waste hybrid composite for food packaging. They found that water uptake decreased by 3.12% with the combination of PLA, nano-silica and Sago pith waste fiber (70:20:10). Opaprakasit et al. [5] were interested in blending PLA with 0.5 wt% of micro-size silica whose surface was coated with a surfactant. An increase in water vapor permeability of PLA composite was observed. They stated that this enhanced water vapor permeability was due to formation of voids resulting from poor compatibility between the silica particles and the PLA matrix. However, it was found that inorganic compounds mixed with polymers have limitations. It is difficult to mix inorganic compounds with polymers due to the different polarities of the materials, affecting dispersion and surface adhesion between particles

*Corresponding author. Tel.: +6689 422 0455
Email address: ksomja@kku.ac.th
doi: 10.14456/easr.2019.32

of inorganic compounds and the polymer matrix. This prevents the desirable performance of nanocomposite materials. Furthermore, most of the packaging was created with petroleum-based materials that are not environmentally friendly.

Recently researchers have been interested in studying biodegradable polymers such as PLA since this bio-polymer can be composted. PLA also has outstanding mechanical strength, similar to petroleum-based polymer materials. However, PLA has a limitation in that it is a polar polymer with a high solubility to moisture, thus causing easy water vapor penetration through the biodegradable polymer film [6]. To increase the performance of packaging products, some researchers studied the properties of PLA nanocomposites in preventing gas and water vapor permeation [6-8], especially for food packaging applications. These studies revealed that water vapor permeability values were reduced by 20 percent [9], 33 percent [7], 45 percent [6], and up to 60 percent [10] depending on the type, quantity, dispersion characteristics and the aspect ratio of nanoclay mixed in PLA. According to Rhim et al. [7], an improvement of water vapor barrier properties of up to 33% was observed for PLA/Cloisite 20A nanocomposites upon addition of 13 wt% of Cloisite 20A. Furthermore, Thellen et al. [11] studied the influence of montmorillonite nanoclay on a PLA matrix. Here, a nanocomposite film was formed using a film blowing process. It was found that addition of 5 wt% of nanoclay could improve the water vapor barrier characteristic by 50% compared to PLA alone. Similar results were observed by Zenkiewicz and Richert [10] who found that with the co-addition of 5 wt% of nanoclay and 20 wt% of PMMA increased the water vapor barrier properties of PLA by up to 60 %. Moreover, it was found that there were other factors that affected gas or vapor barrier properties, such as water solubility, the polymer glass transition temperature (T_g), crystallinity, and hydrolysis reactions. These are factors that easily contribute to the degradation of this biopolymer [12].

The study of the properties of gas and water vapor permeability through nanocomposite polymer films is generally understood using the principle called tortuosity, in which the gas or liquid molecules spend additional time and distance while moving through the film due to the presence of particles of nanoclay or other fillers that act as barriers [6, 13]. Based on a recent literature study, most published work has paid attention to the improvement of water barrier property of PLA composites with the addition of single component fillers. There are very few works focusing on blending PLA polymer with two types of fillers (hybrid filler) with different morphological characteristics. Therefore, to improve the performance of this material, the purpose of the current work is to investigate water vapor transmission through a PLA film containing two different types of fillers. Nanoclay layered double hydroxide (LDH) and silica from rice husk ash were chosen as two component fillers in the present study. Thus, the study examines how nanoclay and silica concentrations and their dispersion characteristics affect the water vapor barrier properties of poly(lactic acid). PLA/silica from rice husk ash/nanoclay hybrid composite films containing 3-10 wt% LDH nanoclay and 3wt% of silica from rice husk ash were prepared using a solvent casting method. The morphology and water vapor transmission rates of these nanocomposites were investigated. X-ray diffraction and transmission electron microscopy were used to examine the alignment and dispersion state of the clay platelets. Additionally, the surface characteristics of PLA nanocomposite films were probed using scanning electron microscopy. Water vapor barrier properties of PLA nanocomposite films were determined by measuring water vapor transmission rates (WVTR) through the films.

2. Materials and methods

2.1 Materials

The poly(lactic acid) used (PLA 4043D) in this work was semi-crystalline with an average D-lactide content of 1.4 wt%, a melting point temperature range of 155–170 °C and molecular weight of 150,000. It was purchased in pellet form from Nature Works, USA. The nanoclay (Tradename: Perkalite; LD grade) was a Mg-Al layered double hydroxide (Mg-Al LDH). It was supplied by Akzo Nobel Polymer Chemicals, Netherlands. Rice husks were collected in Khon Kaen Province, Thailand. All of chemical reagents including sodium dodecyl sulfate (SDS, $C_{12}H_{25}SO_4Na$, Loba Chemie, India), hydrochloric acid (37% w/w, Sigma-Aldrich), sodium hydroxide and dichloromethane (ACI Labscan, Thailand), were of analytical grade and used as received. Deionized water (DI water) was used throughout the experiment.

2.2 Intercalation of nanoclay Perkalite with dodecyl sulfate (DS)

The surface of LDH nanoclay (Perkalite) was modified by intercalation with dodecyl sulfate (DS) through an anion exchange. This increased the interlayer distance of LDH promoting intercalation of the polymer into the interlayer galleries of organically modified LDH. Anion exchange was carried out in a single step according to the procedure reported by Shabanian et al. [14]. Briefly, 0.10 g of Perkalite was added into 100 ml of a sodium dodecyl sulfate solution (0.06 M) under continuous stirring at 50 ˚C. During the anion exchange reaction, the pH value of the suspension was kept constant at 10±2 by addition of a solution of 1 M of sodium hydroxide (NaOH). The suspension was stirred continuously at the same temperature for 30 min and then the temperature was increased to 75 ˚C for 18 h. Finally, an insoluble solid product was collected by filtration and washed with DI water until the pH of the supernatant solution was close to 7. The final product was then dried in a vacuum oven at 80 ˚C until a constant weight was obtained. The obtained product is an organically modified Perkalite denoted as PKL_DS. Particle size analysis of PKL_DS nanoclay was performed using a N_2 adsorption – desorption apparatus (ASAP 2460, Micromeritics, USA). It was found that the average particle size was 363.99 nm with surface area 16.48 m^2/g.

2.3 Preparation of silica rice husk ash

Silica rice husk ash was prepared from rice husks using acid pretreatment followed by incineration. The procedure was previously reported [15-16]. Approximately 20 g of rice husk was mixed with 50 ml of 1 M hydrochloric acid under magnetic stirring for 3 h at room temperature. It was then washed with DI water to remove the hydrochloric acid. Residue from the acid pretreated rice husk was dried at 80 ˚C for 2 h in an oven and subsequently incinerated at 600 ˚C for 1 h in a muffle furnace. The brown residue became white in color, indicating silica formation. The obtained white powder was washed with DI water several times to remove the hydrochloric acid and then dried

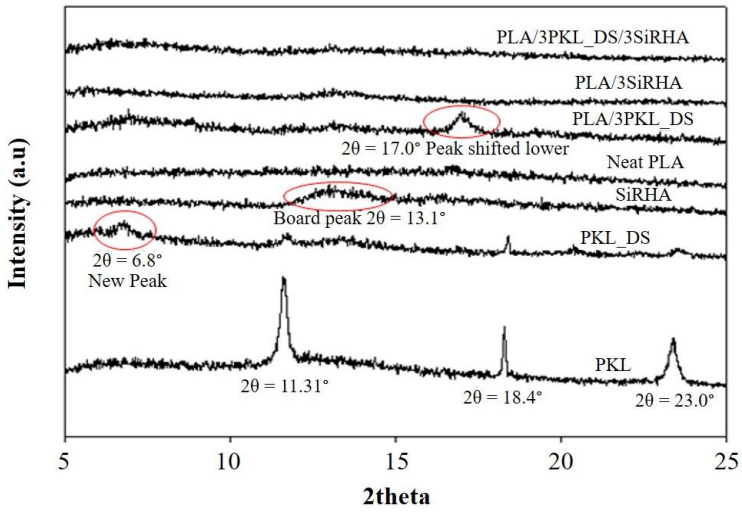

Figure 1 XRD patterns of nanoclay PKL, PKL_DS, SiRHA, neat PLA, PLA/3PKL_DS, PLA/3SiRHA and PLA/3PKL_DS/3SiRHA nanocomposite films.

in an oven at 50 ˚C for 24 h. It was ground in a crucible to a fine particle size and then kept in a desiccator to avoid moisture absorption. This final white powder was silica rice husk ash and was denoted as SiRHA. The particle size and surface area of SiRHA particles were determined by using a N_2 adsorption – desorption apparatus (ASAP 2460, Micromeritics, USA). The average particle size was 50.91 nm with surface area of 117.84 m^2/g.

2.4 Preparation of PLA/SiRHA /PKL_DS nanocomposite films

The PLA/SiRHA/PKL_DS nanocomposite films were prepared by solution casting. First, 5 g of PLA pellets were dissolved in 50 ml of dichloromethane at room temperature under magnetic stirring for 1 h. An appropriate content of SiRHA and PKL_DS fillers were weighed and mixed with the PLA solution under vigorous stirring at room temperature for 4 h. At the end of stirring, the mixture was poured into a 14 cm diameter Petri disk mold and air-dried overnight. The PLA/SiRHA/PKL_DS nanocomposite films were then peeled from the molds. The nanocomposite films obtained had a thickness of about 1.0 mm. They were denoted as PLA/(x)SiRHA /(y)PKL_DS (where x and y are the weight percent loading of SiRHA and PKL_DS filler in the films, respectively). The nanocomposite films were stored in a desiccator until used.

2.5 Characterization techniques

2.5.1 X-ray diffraction

X-ray diffraction spectra (XRD) were collected using a Bruker D8 Advance X-ray diffractometer operating at 45 mA and 33 kV. A bent quartz monochromator was used to select the CuKα radiation (k = 0.15406 nm).

2.5.2 Transmission electron microscopy

Transmission electron microscope (TEM) images were obtained using an FEI Tecnai T12 field-emission electron microscope with an accelerating voltage of 80 kV, with microtomed epoxy-embedded ultrathin samples. The samples were cut using an ultramicrotome equipped with a diamond knife to obtain 60 nm ultrathin sections that were placed on copper grids.

2.5.3 Scanning electron microscopy

The surface morphology of nanocomposite films was investigated using a Hitachi S-3000N (Hitachi, Japan) scanning electron microscope (SEM) operated at an accelerating voltage of 30 kV. The surfaces of the samples were coated with a thin layer of gold prior to observation.

2.5.4 Water vapor transmission rate test

Water vapor transmission rate (WVTR) measurements were performed to determine the water vapor barrier properties of the nanocomposite films. This measurement was done on PLA nanocomposite films with various loadings of PKL_DS filler according to ASTM E96. A commercial Labthink® model PERME W3/0120 apparatus was used at 32 ˚C with 50% relative humidity (50% RH). The thickness of the sample was measured at least ten different positions using micrometer calipers. The average thickness was recorded prior to testing. 20 g of dry silica gel (desiccant) was loaded into a test cup. Samples with an area of 30 cm^2 were sealed in test cups. Each test cup was placed in a chamber at 32 ˚C with 50% RH. The weight of the cup was recorded every 30 min for 24 h or until a constant weight was obtained. The tests were performed in triplicate and the average values were reported. The WVTR values were calculated from the slope of the weight change against time plot using the exposed surface area of the sample in equation (1):

$$WVTR = \frac{Weight\ change}{Area\ x\ time} \qquad (g\ m^{-2}\ day^{-1}) \qquad (1)$$

3. Results and discussion

3.1 Morphological properties

Results of the morphological studies of PKL, PKL_DS, SiRHA, neat PLA film and PLA nanocomposite films conducted by X-ray diffraction (XRD) and TEM are shown in Figures 1 and 2, respectively. The XRD spectra

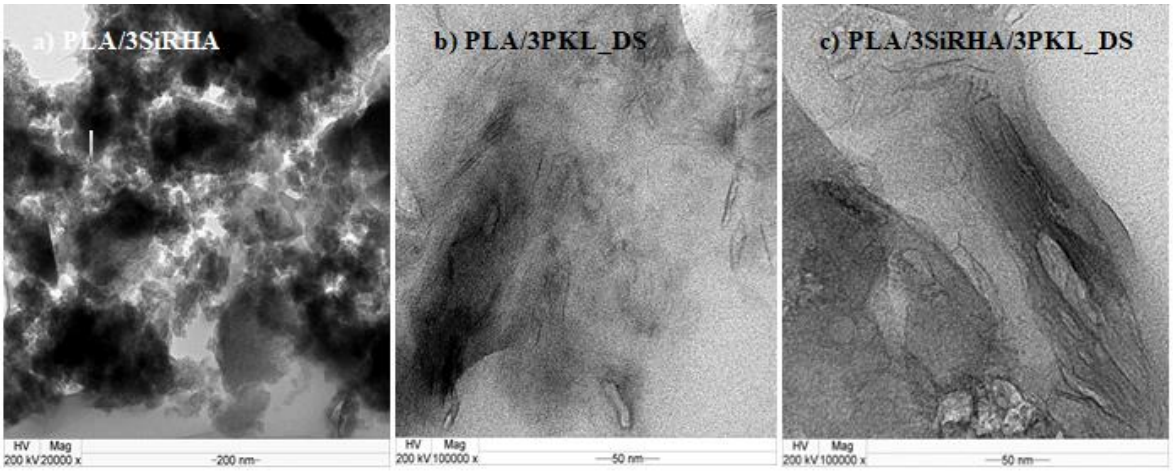

Figure 2 TEM micrographs of a) PLA/3SiRHA, b) PLA/3PKL_DS, c) PLA/3SiRHA/3PKL_DS nanocomposites.

in Figure 1 show no peak for 100% PLA, which indicates that it is an amorphous material. XRD of unmodified PKL exhibits the strongest diffraction peak at $2\theta = 11.31^{\circ}$, corresponding to the reflection of a crystalline form with a basal spacing of 0.78 nm. Other diffraction peaks located at $2\theta = 18.4^{\circ}$ and 23.0° can be ascribed to the crystal structure of layered double hydroxide nanoclay [1, 17]. After organic treatment of layered double hydroxide nanoclay (Perkalite) by anionic exchange with dodecyl sulfate (DS), the X-ray reflections were shifted to a lower angle position and the degree of crystallinity was reduced. In fact, the PKL_DS displays a (0 0 3) diffraction peak at $2\theta = 6.8^{\circ}$ corresponding to an interlayer distance of 1.29 nm, which is much larger than that of the untreated nanoclay PKL [1, 18-19]. The XRD pattern of SiRHA shows that silica from rice hush ash has a broad peak at around $2\theta = 13.3^{\circ}$. This result indicates that SiRHA possesses a non-crystalline structure [16, 20].

The morphology of PLA/3SiRHA, PLA/3PKL_DS and PLA/3SiRHA/3PKL_DS nanocomposite films was determined using XRD and the results are shown in Figure 1. The XRD pattern of PLA/3PKL_DS displays a weak diffraction peak at $2\theta = 17.0^{\circ}$, corresponding to the presence of interlayer distances greater than 0.48 nm [21]. This result suggests that the molecular chains of PLA could have been successfully inserted into and become well-dispersed in the nanoclay PKL_DS interlayers [22-23]. At the 3 wt% level of SiRHA in a PLA nanocomposite film, the XRD pattern exhibited no peak diffraction. The absence of reflection indicates that the material has no crystalline structure. A similar absence of a diffraction peak has been observed in the PLA/3SiRHA/3PKL_DS nanocomposite indicating that the silica and organoclay layered double hydroxide (PKL_DS) may have undergone increased disorder by polymer chain insertion during the film solvent casting process. Moreover the higher order reflection disappears, which implies an increase in the disorder of the interlayer. Alternatively, PLA molecular chains were intercalated in nanolcay interlayers [6, 23].

In order to confirm the dispersion state of PKL_DS and SiRHA, the morphology of nanocomposites of PLA/3SiRHA, PLA/3PKL_DS and PLA/3SiRHA/3PKL_DS was further investigated using TEM. The resulting TEM images are shown in Figure 2. Figures 2a and 2b are TEM images of PLA nanocomposite film containing 3 wt% loading of SiRHA and nanoclay PKL_DS respectively. The average particle size of SiRHA and the average length of nanoclay PKL_DS appearing in TEM images of Figures 2a and 2b were measured from the micrographs by using Image J® software. Based on this determination, the average particle size of SiRHA was 90.63 nm, while the average thickness of the nanoclay PKL_DS platelets in the PLA matrix was 2.7 nm. TEM images of SiRHA and nanoclay PKL_DS clearly show different morphology. SiRHA particles exhibit a sphere-like shape, while nanoclay PKL_DS is a nano-platelet and it appears as very fine solid parallel lines throughout the PLA matrix. Moreover, Figure 2a illustrates the presence of some SiRHA agglomerates reflecting poor dispersion of SiRHA particles in the PLA matrix. In Figure 2b, the TEM micrograph displayed good dispersion of PKL_DS in the PLA matrix. This is likely due to surface modification of nanoclay by dodecyl sulfate. The organic substance helps to expand the interlayer space of nanoclay PKL_DS, allowing for the intercalation of PLA chains into the interlayers of nanoclay PKL_DS, enhancing delamination of nanoclay PKL_DS in the PLA matrix. This resulted in good compatibility between nanoclay PKL_DS and PLA matrix [24]. Surface modification also makes LDH less hydrophilic leading to better dispersion in the PLA matrix [23]. In the case of the PLA/3SiRHA/3PKL_DS nanocomposite, most nanoclay PKL_DS and SiRHA fillers were homogeneously dispersed in the PLA matrix at the nanometer scale. The intercalated nanocomposite structure is shown in more detail in Figure 2c. The lines in the micrograph are the edges of the nanoclay PKL_DS platelets and SiRHA particles. Intercalated stacked layers of PKL_DS coexist in the nanocomposite, implying that the nanocomposite has an intercalated structure [6]. On the basis of XRD and TEM analysis, it can be concluded that intercalated PLA/PKL_DS and PLA/SiRHA/PKL_DS nanocomposites were attained.

3.2 Surface morphology of neat PLA and PLA-matrix nanocomposites

The surface morphology of neat PLA and PLA-based nanocomposite films is shown in SEM images given in Figure 3. The surface of the neat PLA film appears homogeneous and relatively smooth. The film, however, shows signs of brittleness, which is a characteristic of the PLA polymer (Figure 3a). SEM images of PLA nanocomposites containing individual fillers, 3 wt% of SiRHA and 3 wt% of PKL_DS, are shown in Figures 3b and 3c. Figure 3b clearly shows SiRHA agglomerates and phase

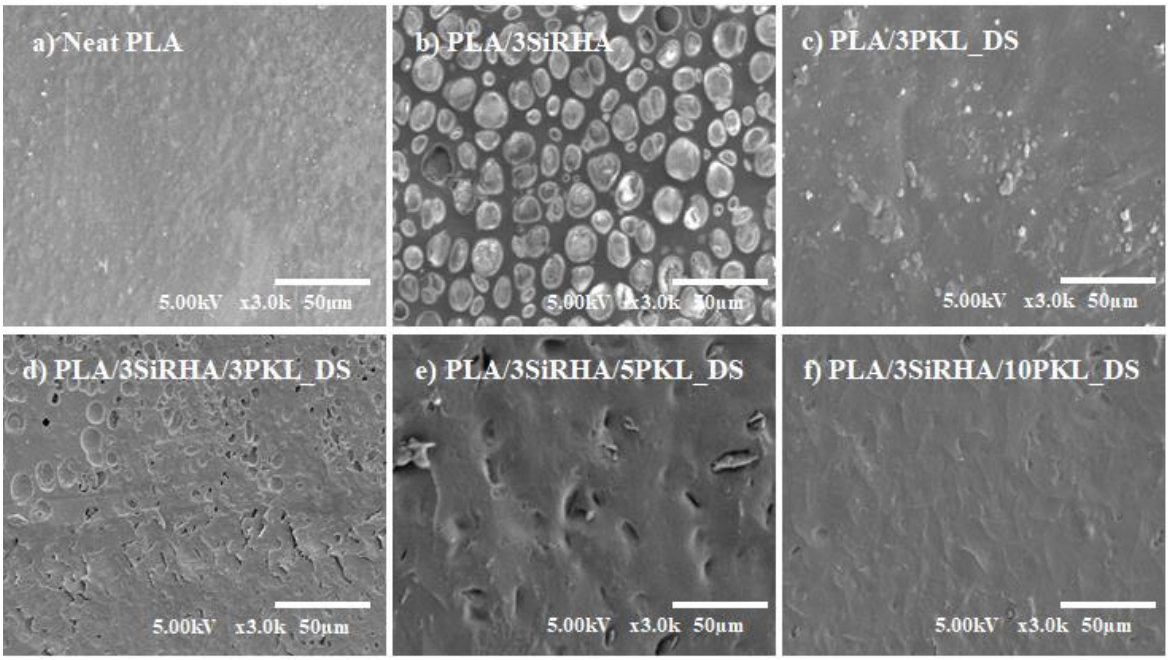

Figure 3 SEM images of a) neat PLA, b) nanocomposites of PLA/3SiRHA, c) PLA/3PKL_DS, d) PLA/3SiRHA/3PKL_DS, e) PLA/3SiRHA/5PKL_DS and f) PLA/3SiRHA/10PKL_DS.

separation of SiRHA in the PLA matrix, suggesting poor bonding between the two phases. Additionally, some holes and cavities are observed on the surface of the PLA/3wt% SiRHA nanocomposite film. These may represent regions where SiRHA particles have been pulled away from the matrix due to debonding of SiRHA particles. This result is consistent with that of Daramola et al. [25], who observed silica agglomerates and poor bonding at the interfaces when silica was added into a high density polyethylene matrix**.** Figure 3c exhibits no phase separation, implying that PKL_DS nanoclay was compatible with PLA matrix. This again was due to the surface modification of nanoclay with dodecyl sulfate (DS). Surface modification enhanced the delamination of LDH, thus good compatibility between PLA matrix and nanoclay LDH resulted. Additionally, surface modification also makes LDH less hydrophilic, enhancing dispersion of nanoclay LDH in PLA. Films containing a constant of 3 wt% SiRHA with various PKL_DS loadings of 3, 5, 10 wt% (Figures 3 d-f) reveal a relatively homogeneous surface with few cavities or holes. The appearance of tiny voids or cavities on the PLA/3SiRHA/3PKL_DS nanocomposite surface (Figure 3d) and PLA/3SiRHA/5PKL DS nanocomposite surface (Figure 3e) was due to the presence of silica, which tends to phase separate from the polymer matrix. It is notable that PKL_DS is well dispersed in the PLA matrix and is very compatible with the PLA matrix, as is evident in Figure 2c. Incorporation of PKL_DS to PLA containing silica increased the homogeneous area of the matrix, contributing to a reduction of SiRHA phase domains. This was more pronounced at a higher loadings of PKL_DS (5 and10 wt%). SEM images of these samples revealed the presence of fewer holes as well as a more homogeneous and smoother surfaces compared to that PLA containing SiRHA alone (Figure 3b). It should also be noted that the matrix phase in Figure 3f (10 wt% PKL_DS with the presence of 3 wt% SiRHA) exhibited a very dense and compact structure. It might be anticipated that the observed structural differences would manifest themselves in the absorption behavior of these nanocomposites.

3.3 Water vapor barrier properties of neat PLA and PLA nanocomposites

Figure 4 shows the water vapor transmission rate (WVTR) of neat PLA and PLA based nanocomposite films with various filler loadings. WVTR is a measurement of the rate of water vapor molecules diffusing through a polymer matrix. As can be seen, all PLA nanocomposite films have lower WVTR than the neat PLA film. From Figure 4, there is a reduction in WVTR with increasing PKL_DS and SiRHA loading. This is attributed to dispersion of PKL_DS nanoclay and the presence of silica from rice husk ash in the film. This increased the length of tortuous pathways for water molecules diffusing through the film. To understand the influence of particle dispersion on the rate of water vapor diffusion through the film, a schematic diagram of a tortuous diffusion model is presented in Figure 5. In the presence of good dispersion, there is overlap among the barriers and a diffusing molecule is forced to go around each layer of filler particles. If dispersion is poor, there are gaps through which the diffusing molecule can pass through the film relatively unhindered. The longer the tortuous pathway, the larger are diffusion times for water vapor molecules through the film. This resulted in a lower WVTR value of both PLA/SiRHA and PLA/PKL_DS films compared to neat PLA film. A maximum reduction of 42% WVTR was achieved for PLA/PKL_DS nanocomposite with 3 wt% PKL_DS loading compared with neat the PLA film. This result is in agreement with data of Duan and coworkers [6], who incorporated 5 wt% of organically modified montmorillonite into PLA and found an improvement of 40% in water vapor barrier properties. The influences of SiRHA filler on the WVTR of PLA nanocomposite films are shown in Figure 4. Addition of 3 wt% SiRHA alone led to a higher WVTR value than that of PLA with 3 wt% PKL_DS loading. This is due to three characteristics of SiRHA particles. First, the specific surface

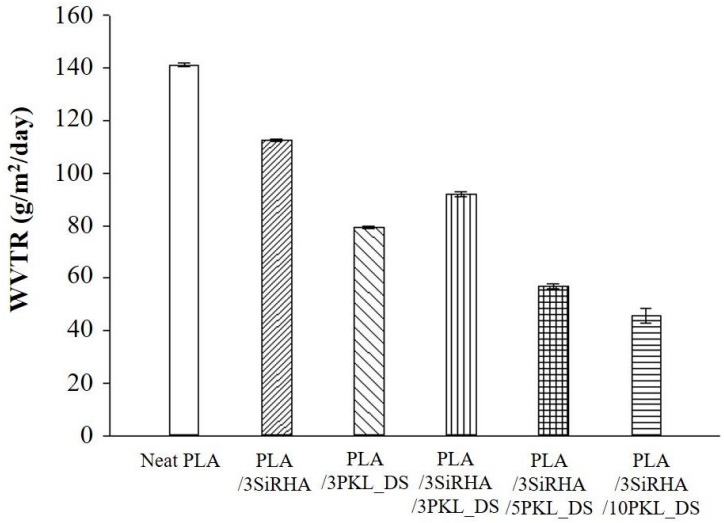

Figure 4 Water vapor transmission rate (WVTR) of neat PLA and PLA based nanocomposites with different PKL_DS, SiRHA and SiRHA/PKL_DS loadings.

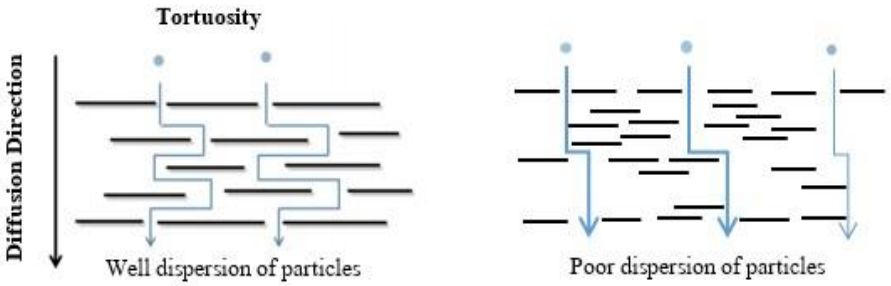

Figure 5 Schematic diagram of tortuous path model modified from [9].

area of SiRHA (117.84 m^2/g) is higher than that of PKL_DS nanoclay (16.48 m^2/g) indicating that SiRHA is relatively more porous than PKL-DS nanoclay. Next, the results of particle size analysis show that the average particle size of SiRHA (50.91 nm) is smaller than PKL_DS (363.99 nm). However, after mixing these fillers into PLA polymers, the TEM images of nanocomposite films showed SiRHA agglomerates (poor dispersion) in the PLA matrix (evidenced from Figure 2a), while PKL_DS showed better dispersion (Figure 2b). Finally, the holes and cavities on the surface of the PLA/3wt%SiRHA nanocomposite film were due to debonding of SiRHA particles from the PLA matrix (evidenced from Figure 3b). The porous structure of SiRHA particle itself, the poor dispersion of SiRHA (induced shorter tortuous pathway) and holes in the nanocomposite film all facilitated diffusion of water vapor molecules through the PLA matrix. This resulted in a higher WVTR for PLA with 3 wt% SiRHA loading than PLA with the same PKL_DS loading. The influence of the incorporation of a combination of PKL_DS and SiRHA in PLA nanocomposites on the WVTR was also investigated and results are illustrated in Figure 4. With incorporation of a constant 3 wt% SiRHA into the nanocomposite films with various PKL_DS loadings, there was a reduction in WVTR when increasing the PKL_DS content from 3 to 5 wt%. This reduction in WVTR might be attributed to the presence of PKL_DS that could seal holes and pores in the structure of the nanocomposite film. A reduction of holes and pores retards water vapor diffusion through a film, resulting in a decreased water permeability [6, 13]. Furthermore, increasing the content of PKL_DS from 5 wt% to 10 wt% further reduced the WVTR to the lowest value, 45 $g/m^2/day$. The result was a 67% improvement of water vapor barrier properties compared with the PLA film alone. This can be explained using the SEM images of Figure 3f, which indicate a dense structure of PLA/SiRHA/PKL_DS nanocomposite film at 10 wt% PKL_DS. The compact structure slows water vapor permeation, thus lowering the WVTR value. Furthermore, the lower porosity and denser characteristics of PKL_DS nanoclay (compared to SiRHA particles) could obstruct water vapor transmission through the film owing to the good dispersion of PKL_DS in the PLA matrix (inducing longer tortuous pathways). Thus, a reduction in the WVTR value was observed, and it was more pronounced at higher PKL_DS loadings. It can be summarized that incorporation of PKL_DS has greater effect on the reduction of WVTR values of nanocomposite films than that of the SiRHA filler. The maximum reduction of the WVTR value was achieved with incorporation of 3 wt% SiRHA/10 wt% PKL_DS. These low WVTR value suggest PLA/3SiRHA/10PKL_DS nanocomposite film as an alternative material for green-based packaging.

4. Conclusions

PLA based nanocomposite films with addition of various levels of SiRHA, PKL_DS and SiRHA/PKL_DS in combination were successfully produced using solvent casting. The addition of PKL_DS in conjunction with SiRHA as co-fillers improved water vapor barrier properties

of the PLA matrix. The results from both XRD and TEM confirmed that the nanocomposite structures were intercalated. The XRD analysis showed that the clay interlayer spacing increased from 0.76 to 1.29 nm. TEM micrographs indicated that the clay particles were well dispersed in the polymer matrix. SEM results revealed the smooth and homogeneous surface of PLA nanocomposite films at 10 wt% PKL_DS loadings. In contrast, a porous structure morphology was observed for PLA with addition of SiRHA alone or SiRHA in combination with a low content of 3 wt% or 5 wt% PKL_DS. However, the porous morphology of the film disappeared when the PKL_DS level was increased to 10 wt% in combination with SiRHA/PKL_DS loading. WVTR values of all PLA based nanocomposites are lower than that of PLA alone, which suggests that incorporation of PKL_DS and SiRHA yields an improvement of water vapor barrier properties over that of pure PLA. A reduction of the WVTR is due to longer tortuous pathways for water molecule diffusion created by fillers. The WVTR of PLA nanocomposites with co-addition of 3 wt% SiRHA/10 wt% PKL_DS was reduced by 67% compared to that of PLA alone. This reflects the potential of using PLA/SiRHA/PKL_DS hybrid nanocomposites as green packaging materials.

5. Acknowledgements

We gratefully acknowledge Khon Kaen University under the Incubation Researcher Project for their financial support.

6. References

[1] Bugatti V, Livi S, Hayrapetyan S, Wang Y, Estevez L, Vittoria V, et al. Deposition of LDH on plasma treated polylactic acid to reduce water permeability. J Colloid Interface Sci. 2013;396:47-52.

[2] Shankar S, Wang LF, Rhim JW. Incorporation of zinc oxide nanoparticles improved the mechanical, water vapor barrier, UV-light barrier, and antibacterial properties of PLA-based nanocomposite films. Mater Sci Eng C. 2018;93:289-98.

[3] Pilić BM, Radusin TI, Ristić IS, Silvestre C, Lazić VL, Baloš SS, et al. Silica nanoparticles as reinforcing filler for poly (lactic acid) matrix. Hem Ind. 2016;70**:**73-80.

[4] Masnar A, Coorey R. Application of sago pith waste and nanosilica from rice husk ash as hybrid bio-nanofiller composites for food plastic packaging. Ukr Food J. 2017;6:618-31.

[5] Opaprakasit P, Boonpa S, Jaikaew N, Petchsuk A, Tangboriboonrat P. Preparation of surface-modified silica particles from rice husk ash and its composites with degradable polylactic acid. Macromol Symp. 2015;354:48-54.

[6] Duan Z, Thomas NL, Huang W. Water vapour permeability of poly(lactic acid). J Membrane Sci. 2013;445:112-8.

[7] Rhim JW, Hong SI, Ha CS. Tensile, water vapor barrier and antimicrobial properties of PLA/nanoclay composite films. LWT-Food Sci Techno. 2009;42:612-7.

[8] Pantani R, Gorrasi G, Vigliotta G, Murariu M, Dubois P. PLA-ZnO nanocomposite films: vapor barrier properties and specific end-use characteristics. Eur Polym J. 2013;49:3471-82.

[9] Tan B, Thomas NL. Tortuosity model to predict the combined effects of crystallinity and nano-sized clay mineral on the water vapour barrier properties of polylactic acid. Appl Clay Sci. 2017;141:46-54.

[10] Zenkiewicz M, Richert J. Permeability of polylactide nanocomposite films for water vapour, oxygen and carbon dioxide. Polym Test. 2008;27:835-40.

[11] Thellen C, Orroth C, Froio D, Ziegler D, Lucciarini J, Farrell R, et al. Influence of montmorillonite layered silicate on plasticized poly (L-lactide) blown films. Polymer. 2005;46:11716-27.

[12] Shogren R. Water vapor permeability of biodegradable polymers. J Environ Polym Degrad. 1997;5:91-5.

[13] Nielsen LE. Models for the permeability of filled polymer systems. J Macromol Sci Pure Appl Chem. 1967;5:929-42.

[14] Shabanian M, Basaki N, Khonakdar HA, Jafari SH, Hedayati K, Wagenknecht U. Novel nanocomposites consisting of a semi-crystalline polyamide and Mg-Al LDH: morphology, thermal properties and flame retardancy. Appl Clay Sci. 2014;90:101-8.

[15] Athinarayanan J, Periasamy VS, Alhazmi M, Alatiah K.A, Alshatwi AA. Synthesis of silica nanoparticles from rice husks for biomedical applications. Ceram Int. 2015;41:275-81.

[16] Sankar S, Sharma SK, Kaur N, Lee B, Kim DY, Lee S, et al. Biogenerated silica synthesized from sticky, red, and brown rice husk ashes by a chemical method. Ceram Int. 2016;42:4875-85.

[17] Livi S, Bugatti V, Estevez L, Rumeau JD, Giannelis EP. Synthesis and physical properties of new layered double hydroxides based on ionic liquids: Application to a polylactide matrix. J Colloid Interface Sci. 2012;388:123-9.

[18] Pan P, Zhu B, Dong T, Inoue Y. Poly(L-lactide)/layered double hydroxides nanocomposites: preparation and crystallization behavior. J Polym Sci B. 2008;46:2222-33.

[19] Alamri H, Low IM, Alothman Z. Mechanical, thermal and microstructural Characteristics of cellulose fibre reinforced epoxy/organoclay nanocomposites. Composites Part B. 2012;43:2762-71.

[20] Fang G, Li H, Chen Z, Liu X. Preparation and properties of palmitic acid/SiO_2 composites with flame retardant as thermal energy storage materials. Sol Energy Mater Sol Cells. 2011;95:1875-81.

[21] Elbasuney S. Surface engineering of layered double hydroxide (LDH) nanoparticles for polymer flame retardancy. Powder Technol. 2015;277:63-73.

[22] Chiang MF, Wu TM. Synthesis and characterization of biodegradable poly(L-lactide)/layered double hydroxide nanocomposites. Compos Sci Technol. 2010;70:110-5.

[23] Chiang MF, Wu TM. Preparation and characterization of melt processed poly(L-)/layered double hydroxide nonocomposites. Composites Part B. 2012;43:2789-94.

[24] Basu D, Das A, Stockelhuber KW, Wagenknecht U, Heinrich G. Advances in layered double hydroxide (LDH) - based elastomer composites. Prog Polym Sci. 2014;39:594-626.

[25] Daramola OO, Oladele IO, Adewuyi BO, Sadiku R, Agwuncha SC. Thermal, structure and morphological properties of high density polyethylene matrix composites reinforced with submicron agro silica particles and titania particles. J Taibah Uni Sci. 2017;11(4):645-53.